PFC/RR-81-22

STUDIES OF PHOTONUCLEAR NEUTRON EMISSION DURING THE START-UP PHASE OF THE ALCATOR C TOKAMAK

D. S. Pappas, R. Furnstahl
G. P. Kochanski

Plasma Fusion Center
Massachusetts Institute of Technology
Cambridge, MA 02139

May 1981

This work was supported by the U.S. Department of Energy Contract No. DE-AC02-78ET51013. Reproduction, translation, publication, use and disposal, in whole or in part by or for the United States government is permitted.

ABSTRACT

Alcator C operations commenced with discharge cleaning and tokamak operation using hydrogen filling gas. Prior to and during these experiments no deuterium gas was allowed into the device. The earliest operation resulted in dosimeter readings of a few Roentgen per shot in the vicinity of the limiter and a localized source of neutron emission of up to 10^9 neutrons/shot. A strong correlation of the neutron emissions with hard X-ray emissions from the limiter and non-thermal features on the synchrotron emissions was observed during these discharges. Gamma energy spectroscopy of the activated limiter after removal from Alcator allowed identification of 16 radioisotopes which were consistent with photonuclear processes (γ,n , γ,p , γ,α reactions) arising in the limiter. After seven months of hydrogen operation conditions were achieved that resulted in substantially less non-thermal activity. Typical neutron emission rates of equal to or less than 10^6 n/sec were observed, i.e., about four orders of magnitude less than the expected D-D thermonuclear neutron emission rates for the same type of discharges if D_2 was used as the filling gas. These results confirm previous measurements performed on the Alcator A tokamak [1].

1. INTRODUCTION

Studies of neutron emissions in present day fusion devices have gained wide acceptance as being an important aid in the understanding of processes that take place in fusion grade plasmas. In both ohmically heated and supplementary heated (neutral beam and RF heated) deuterium plasmas, the neutron emission provides a measure of the fusion reactivities. Furthermore, the emissions can be used to deduce ion temperatures, a technique that has in general been found to be in good agreement with standard ion temperature diagnostics, i.e., charge exchange and Doppler broadening techniques.

A prerequisite for the validity of the neutron deduced ion temperature determinations lies in the certainty that the measured neutron emissions are due to thermonuclear processes, since it is known that significant contributions to the total neutron emissions can be due to non-thermonuclear processes [2,3,4,5]. The dominant sources of spurious neutron emissions in present day tokamak devices result from electrodisintegration or photodissociation processes [6].

The reactions for these processes are given by

$D(e,e'n)H$ threshold = 2.2 MeV (Volume process)

$^{97}Mo(\gamma,n)^{96}Mo$ threshold = 6.8 MeV (Localized process)

The former process results when runaway electrons (whose energies exceed the binding energy of the deuteron) confined in the plasma volume interact with deuterons or impurities, thus producing a non-localized source of neutron emission. The cross section for this process is rather small [7] and the presence of measureable e-d neutron emissions are expected when large fluxes of photonuclear emissions are present. The photonuclear effect arises when runaway electrons that are poorly confined collide with the plasma limiter. In the latter expression above, molybdenum is used as the target atom since molybdenum is used as the limiter material in Alcator C. Photodisintegration processes occur in other materials as well and it has been found that the photonuclear yields scales roughly with Z for a given incident electron energy for thick targets [8]. Photonuclear processes in tokamaks are thus localized at the plasma limiter and are independent of the filling gas used.

In this report we describe studies of the neutron emissions which arose from the photodisintegration process. The measurements were made during the start-up phase of Alcator C using hydrogen fill gas alone. Deuterium gas was not introduced into the machine prior to these experiments to ensure that electrodisintegration or fusion neutron emissions would not contribute to the measured neutron flux.

During this period these emissions were observed and identified, and ultimately we were able to control the rates

of emission such that they were roughly four orders of magnitude less than the expected thermonuclear yields for future comparable discharges, having deuterium as the filling gas.

2. EXPERIMENTAL DESCRIPTION

The design parameters for Alcator C are given in Table 1.

R	a	B_T(max)	I_p(max)	n_o	$T_i \simeq T_e$
64 cm	17 cm	14T	1 MA	2×10^{15} cm^{-3}	1.5 keV

Table I

For the experiments reported here the machine was generally operated at plasma currents of approximately 400 KA and toroidal magnetic fields of 6 T.

Figure 1 shows a schematic view of Alcator C. The system is completely surrounded by a liquid nitrogen cryostat. The Bitter magnet winding which provides the high magnetic field capability almost completely surrounds the vacuum vessel. Three long counter assemblies are placed about the device for the neutron flux measurements. Within each of the three assemblies are placed three BF_3 proportional counters in order to cover a broad range of rates of neutron emission. The two side assemblies are separated by 180° toroidally, one of which is adjacent to the limiter port,

the other on the opposing side of the device. A radionuclide neutron source (PuBe) placed inside the limiter port resulted in a 30 times larger count rate registered by the limiter port long counter than as registered by the long counter on the opposing side of Alcator. Thus it was expected that a localized source of neutron emission which could arise during plasma operation would be easily recognizable as such. The upper long counter assembly was used for determination of the absolute rates of neutron emission. This assembly was calibrated using a PuBe neutron source and a Cf^{252} neutron source. For each calibration the source was placed within the torus and moved along the major and minor axis of Alcator C to simulate a spatially (or localized) distributed source of neutron emission as would be expected in tokamak operation.

3. RESULTS

3.1 Evidence that suggests that the neutron emissions observed were of photonuclear origin is described below.

1. Localization of the neutron emission. Figure 2 shows the outputs of the two side long counters (each voltage spike corresponds to a single neutron event in the detector). The data shows that the limiter long counter registers a significantly larger neutron flux than the opposing long counter, thus indicating that the neutron

emission was localized in the vicinity of the limiter. The digital display of the neutron events was routinely used in the early operations as a check that the events were not due to hard X-ray emissions (i.e., by using pulse height analysis).

2. Correlations of Neutron Emissions with Hard X-Ray Emissions and Synchrotron Emissions. Figure 3 shows the neutron rate (in analog form) as measured by the calibrated top long counter. The maximum neutron rate (at the end of the discharge) was about 10^9 neutrons/sec. This type of discharge was routinely accompanied by a large flux of perpendicular hard X-ray emissions and by non-thermal features in the synchrotron emissions (early in the discharge as indicated by the arrows in the figure). Forward (or energetic) hard X-ray emissions rates (not shown in the figure) also showed a strong correlation with the neutron emissions.

3. Limiter Activation and Analysis. A schematic view of the molybdenum limiter is shown in Figure 4. It consists of twenty separate segments of molybdenum supported by two stainless steel support arms. The lower portion of the figure shows the activated portion of the limiter three days after the last tokamak operation.

A γ spectrum of the sample was then performed using a Ge(Li) diode and several peaks in the spectrum were observed. Analysis of these peaks resulted in identification of sixteen radionuclides as shown in Figure 5. Table 2

shows the isotopic percentages of natural molybdenum.

Isotope	M_o^{92}	M_o^{94}	M_o^{95}	M_o^{96}	M_o^{97}	M_o^{98}	M_o^{100}
Percent Abundance	15.86	9.12	15.7	16.5	9.45	23.75	9.62

Table II

Shown in Figure 6 are some of the possible schemes for γ,n , γ,p and γ,α reactions in molybdenum. The resulting radionuclides from these decay schemes [9] were then compared with the identified radioisotopes from the measured γ-spectrum and it was concluded that the limiter activation was consistent with photodisintegration (of molybdenum) processes.

3.2 Reduction of photonuclear neutron emission.

It has been reported elsewhere [10] that runaway electrons are born very early in the evolution of tokamak discharges. Consistent with these findings we observed that minor disruptions early in the discharge formation resulted in low levels of photonuclear neutron emission, low levels of hard X-ray emission and little or no non-thermal structure in the synchrotron emissions. An example of this type of discharge is shown in Figure 7. Since this was not the most practical way to reduce runaway activity and hence photoneutron emission, another method was attempted. During the latter period that these experiments were carried out, machine operation became more reliable and tests were

performed to adjust the pulsed gas injection time in order that the density rise would occur at the earliest time without causing disruptions in the discharge. It was felt that large density levels very early in the discharge would reduce runaway production and hence photonuclear levels would be lessened. The contrast between early and late gas puffing (3 m-sec difference in the density rise) for similar discharges is shown in Figures 8 and 9 respectively. Reductions in the neutron and hard X-ray emissions are clearly shown in the case of the early gas injection (early density rise case). Subsequent operations resulted in further reductions in photonuclear activity by fine tuning of the gas injection system. Photonuclear rates thereafter were less than 10^6 neutrons/sec. A typical example of this type of discharge is shown in Figure 10.

4. CONCLUSIONS

Rates of neutron emissions of up to 10^9 neutron/shot were observed in hydrogen discharges during the start up phase of Alcator C. Prior to and during these experiments deuterium gas was not let into the machine. Localization of the neutron emission together with radioisotopic analysis of the limiter and correlations with non-thermal phenomena in the plasma indicate that the neutron emissions were of photonuclear origin, i.e., due to photodisintegration of molybdenum nuclei due to Bremsstrahlung production by electron impact. The runaway electron production was

observed to be controllable at times early in the discharge by either minor disruptions or early pulse gas injection. The latter technique was used routinely during the latter part of the experiments and the observed photonuclear neutron rates were typically less than 10^6 neutrons/sec. The low levels of photoneutron emission in these experiments confirm previous measurements performed on the Alcator A tokamak which indicated that low levels of photoneutron emission were obtainable in a high field tokamak.

ACKNOWLEDGEMENTS

The authors wish to thank R. R. Parker and the entire Alcator Group for their support, encouragement and help during the course of this work. We also thank I. H. Hutchinson for sharing the cyclotron emission data. We also gratefully acknowledge E. Karaian and P. Coggio of the M.I.T. Reactor Radiation Protection Group for performing the gamma scan of the Alcator C limiter.

REFERENCES

1. Pappas, D., Parker, R., M.I.T. Report PFC/RR-78-5 (1978).
2. Rose, B., Taylor, A. E., Wood, E., Nature 181 (1958) 1630.
3. Alcator Group, Plasma Physics and Controlled Nuclear Fusion Research 1974 (Proc. 5th Int. Conf. Tokyo, 1974) IAEA (1975) 1, 191.
4. TFR Group, Phys. Lett. 60 A (1977) 219.
5. Strachan, J., Messervey, E., Stodiek, W., Naumann, R., Girshick, F., Nucl. Fusion 17 (1977) 140.
6. Equipe TFR, Nucl. Fusion 18 (1978) 647.
7. Harder, D., Mehling, R., England, A., Phys. Lett. 32B (1970) 610.
8. Barber, W., George, W., Phys. Rev. 116, 1551 (1959).
9. Lederer, C., Hollander, J., Perlman, I., 'Table of Isotopes' Sixth Edition, Wiley (1967).
10. Knoepfel, H., Spong, D., Nucl. Fusion 19 (1979) 785.

FIGURES

Figure 1. The Alcator C device.

Figure 2. Digital output of the two side port long counters showing localization of neutron emission at the limiter. Neutron rate at the end of the shot $\simeq 10^9$ n/sec.

Figure 3. Analogue display of neutron emission as registered by the top long counter. The neutron emission was typically accompanied by large flux of hard X-ray emission and non thermal features of the cyclotron emission.

Figure 4. Top- schematic view of the segmented molybdenum limiter. Photograph shows the activated region (dark shiny region in center).

Figure 5. Gamma spectrum of the activated region. 16 peaks are identified as shown.

Figure 6. Thick target bremsstrahlung resulting from run-away electrons colliding with the limiter can produce photoneutrons by some of the above reactions. Various unstable isotopes that are produced can be identified by gamma spectrum of the activated sample.

Figure 7. Photoneutron and hard X-ray emission is reduced significantly by a minor disruption early in the discharge. Correspondingly, the non thermal features in the cyclotron emission spectra are reduced.

Figure 8. Early pulse gas injection reduces hard X-ray emission and photoneutron production.

Figure 9. Late pulse gas injection results in increased levels of photoneutron production and hard X-ray emission.

Figure 10. Proper programming of the density rise early in the discharge results in photoneutron rates from 3-4 orders of magnitude less than the expected thermonuclear fusion neutron rates from comparable deuterium discharges. Hard X-ray levels and non thermal features in the cyclotron emission spectra are strongly reduced.

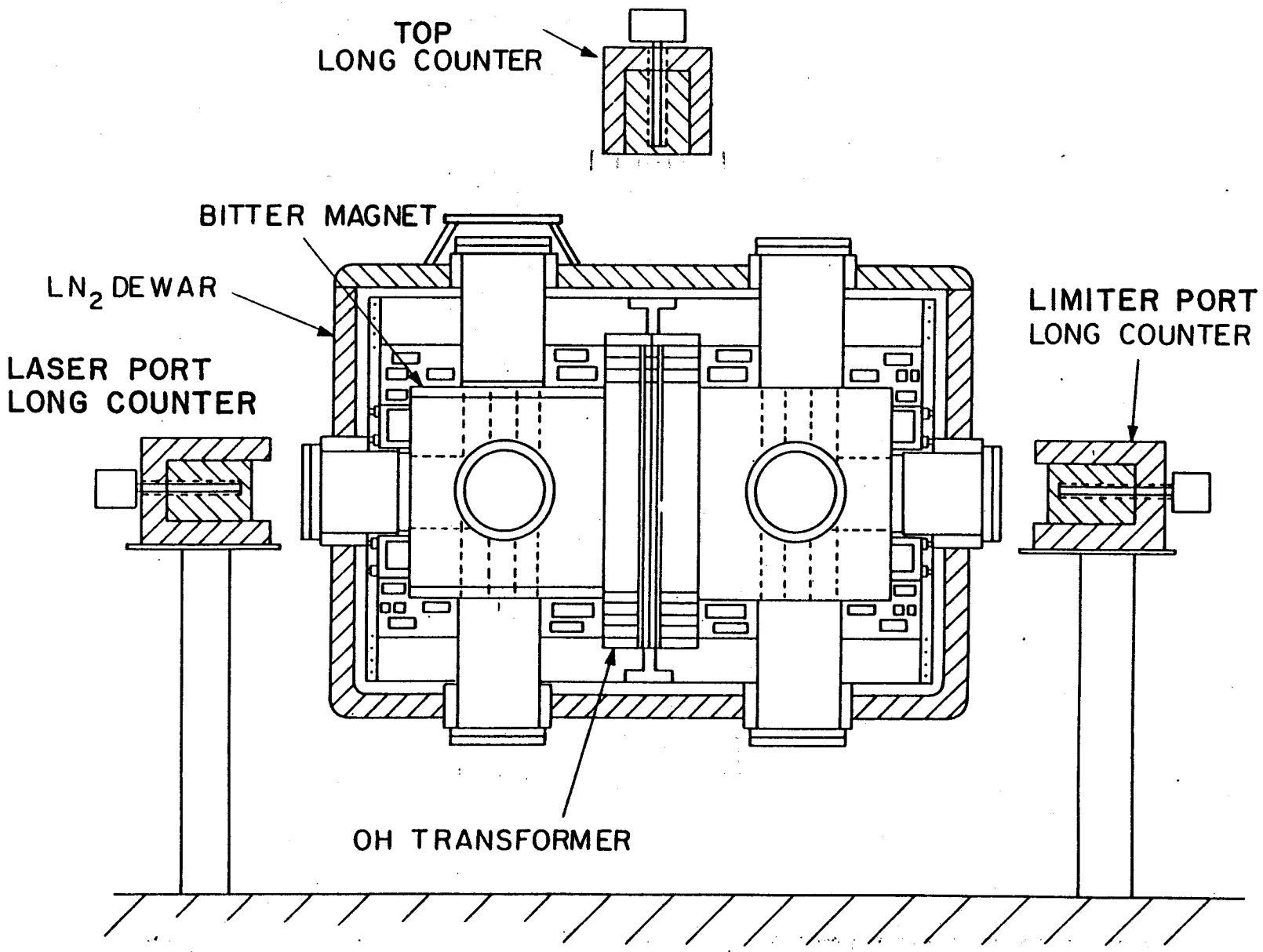
TOP
LONG COUNTER
BITTER MAGNET
LN_2 DEWAR
LASER PORT
LONG COUNTER
LIMITER PORT
LONG COUNTER
OH TRANSFORMER

Figure I.

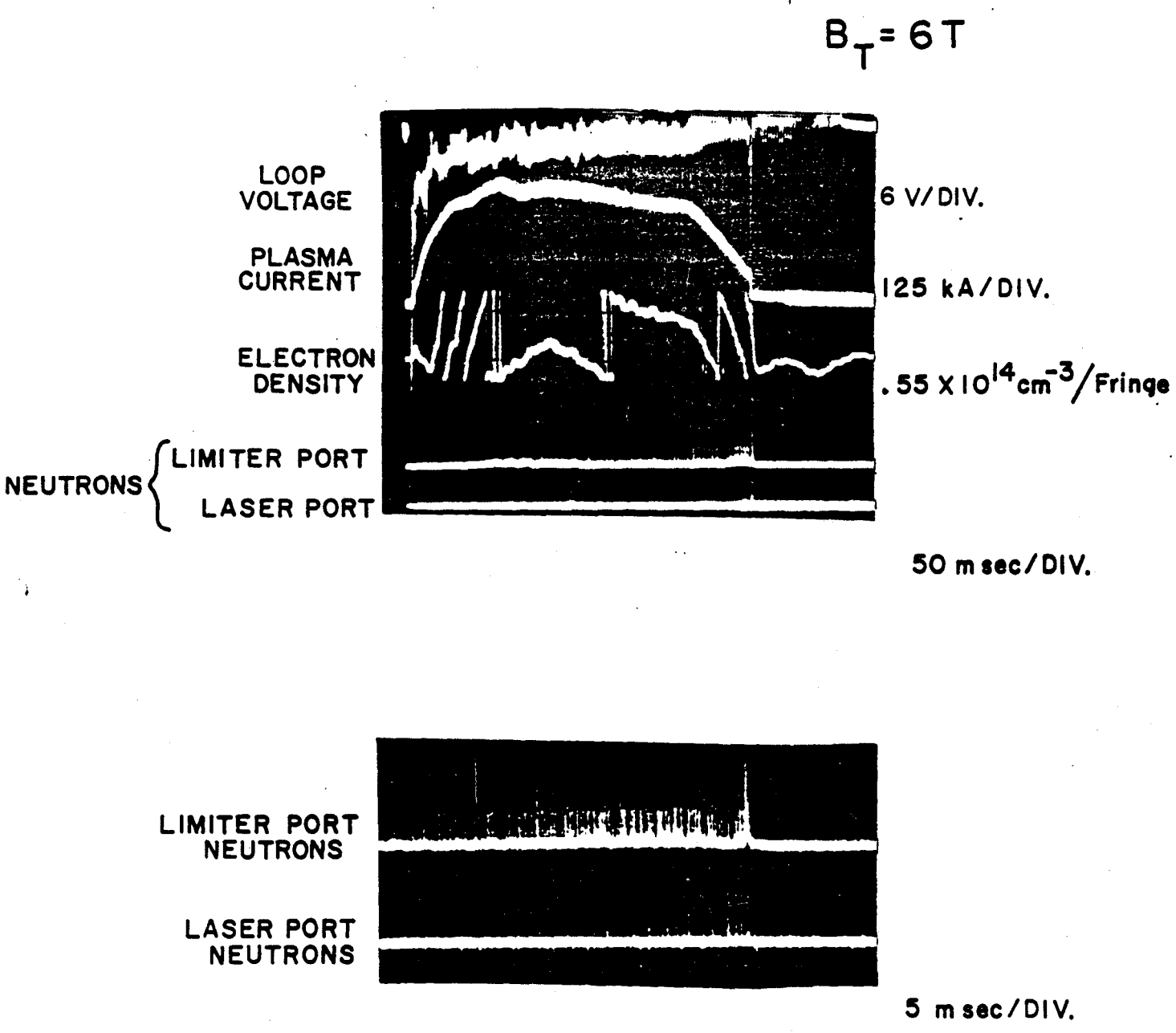
$B_T = 6\,T$
LOOP VOLTAGE
6 V/DIV.
PLASMA CURRENT
125 kA/DIV.
ELECTRON DENSITY
$.55 \times 10^{14} cm^{-3}$/Fringe
NEUTRONS
LIMITER PORT
LASER PORT
50 m sec/DIV.
LIMITER PORT NEUTRONS
LASER PORT NEUTRONS
5 m sec/DIV.

Figure 2

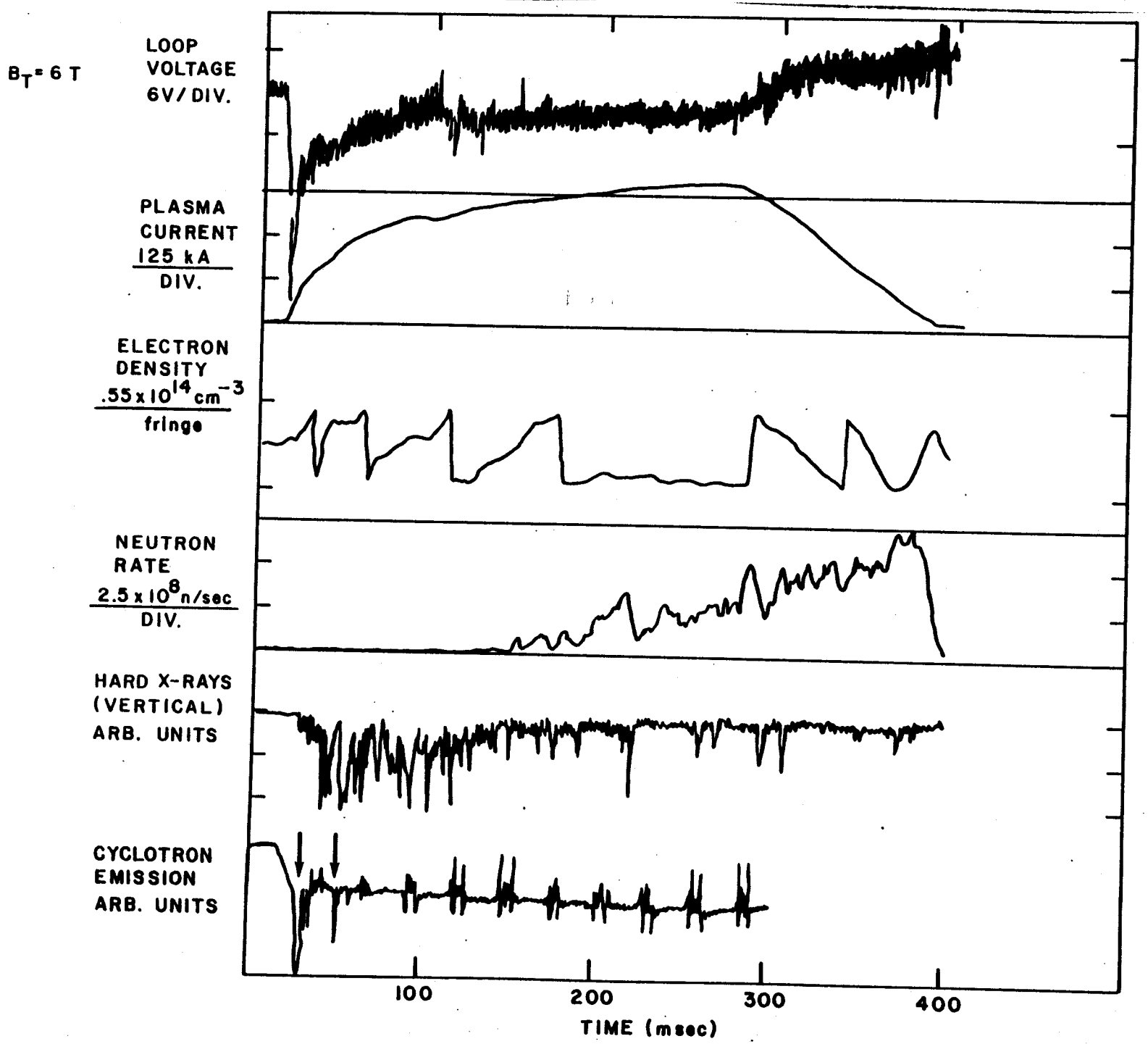
B_T = 6 T
LOOP VOLTAGE 6V/DIV.
PLASMA CURRENT 125 kA / DIV.
ELECTRON DENSITY .55x10^14 cm^-3 / fringe
NEUTRON RATE 2.5x10^8 n/sec / DIV.
HARD X-RAYS (VERTICAL) ARB. UNITS
CYCLOTRON EMISSION ARB. UNITS
100
200
300
400
TIME (msec)

Figure 3

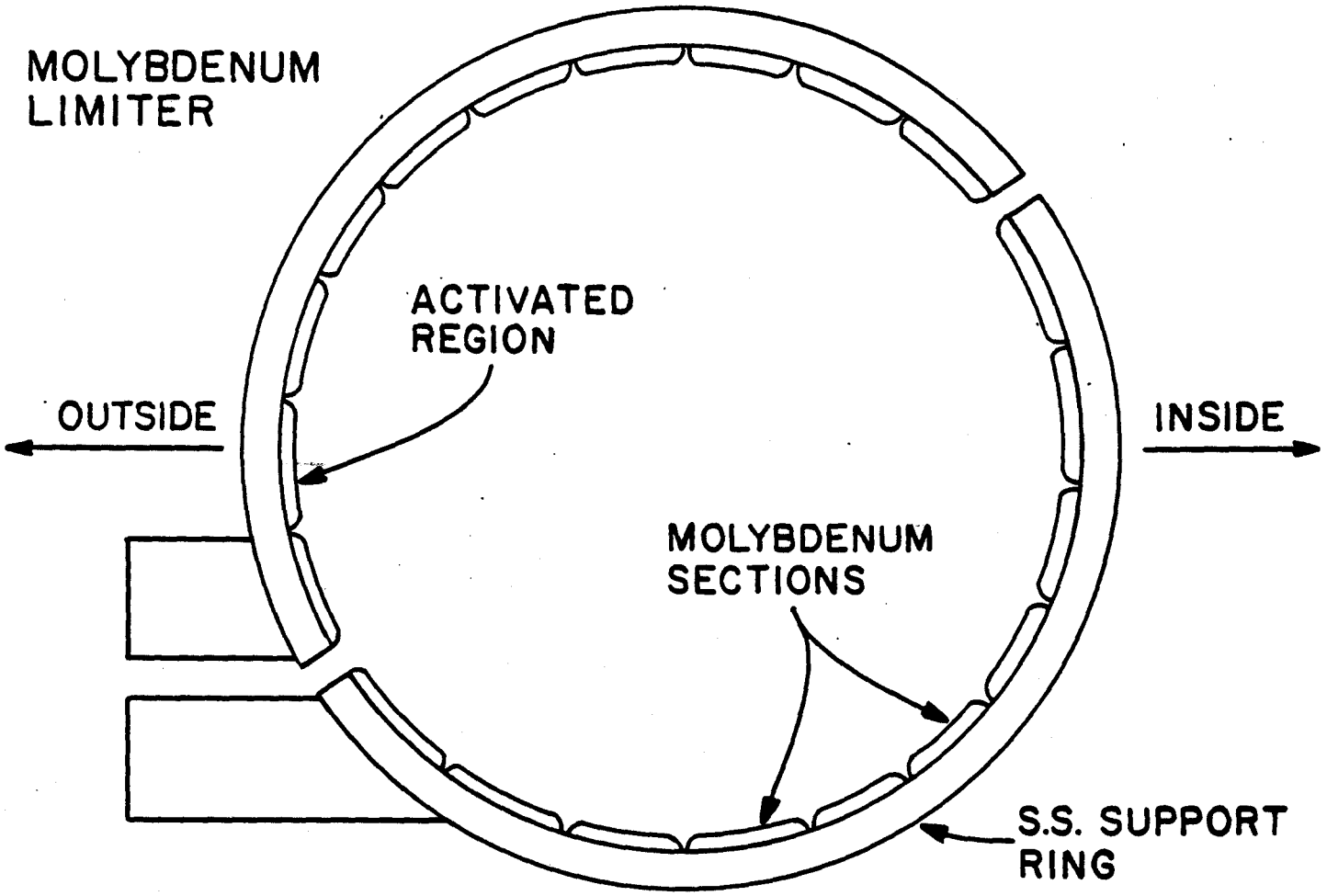
MOLYBDENUM
LIMITER
ACTIVATED
REGION
OUTSIDE
INSIDE
MOLYBDENUM
SECTIONS
S.S. SUPPORT
RING

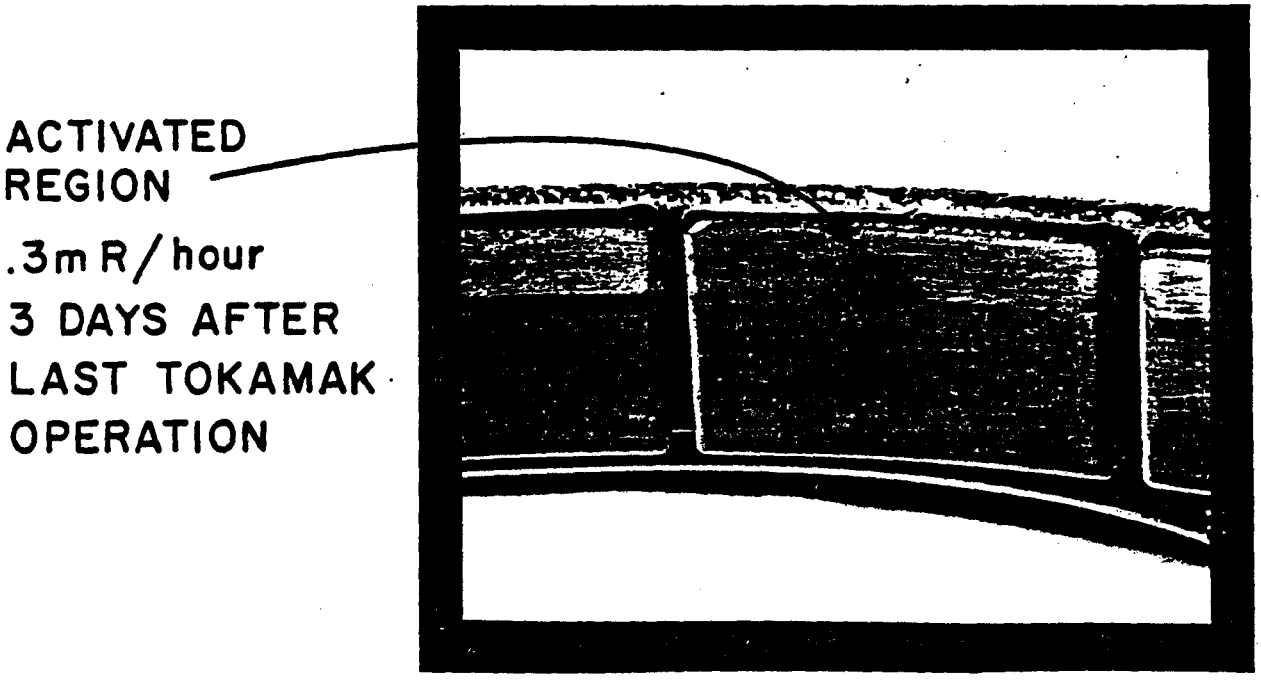
ACTIVATED
REGION
.3m R/hour
3 DAYS AFTER
LAST TOKAMAK
OPERATION

Figure 4.

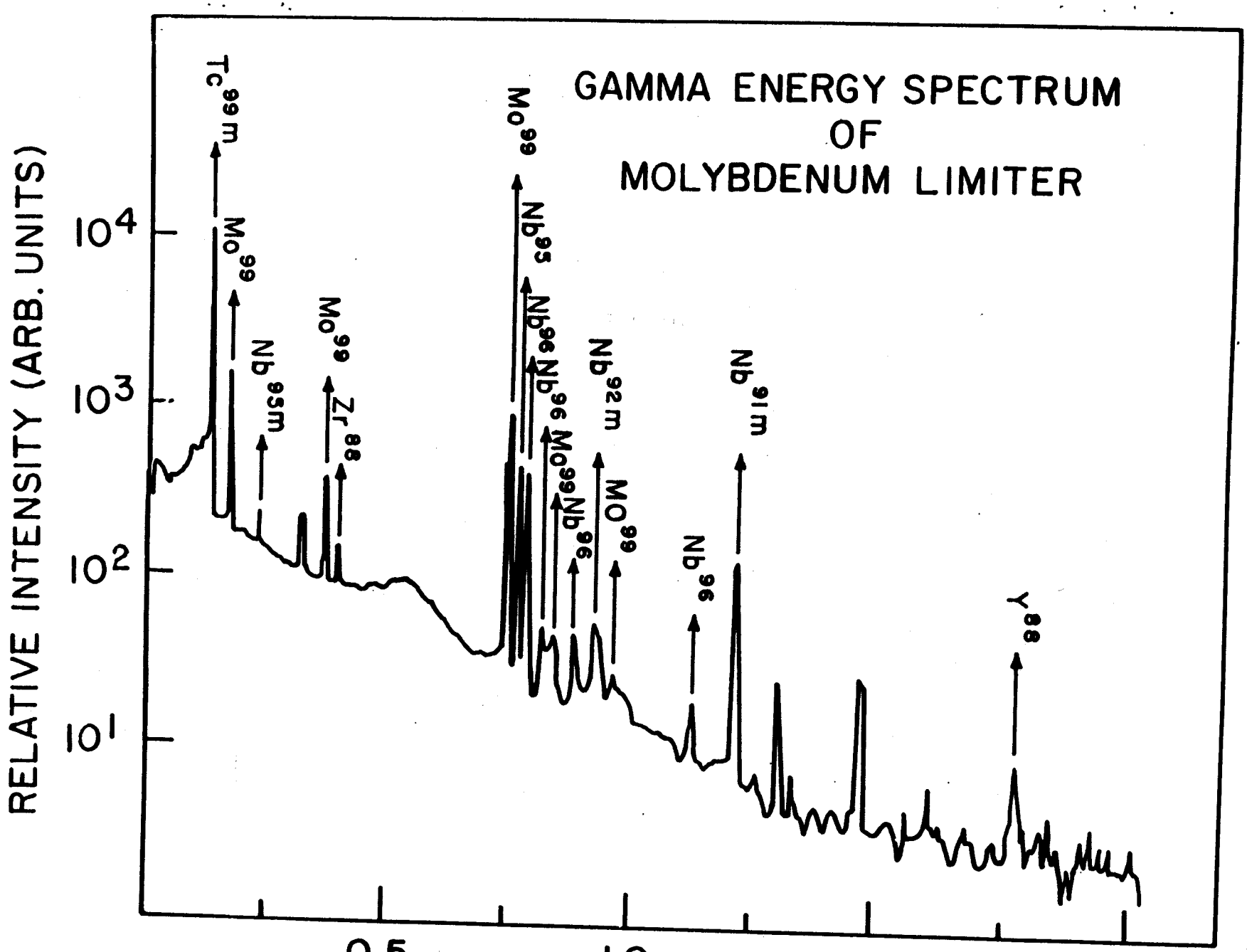
GAMMA ENERGY SPECTRUM
OF
MOLYBDENUM LIMITER
RELATIVE INTENSITY (ARB. UNITS)
10^4
10^3
10^2
10^1
Tc^{99m}
Mo^{99}
Nb^{95m}
Mo^{99}
Zr^{88}
Mo^{99}
Nb^{95}
Nb^{96}
Nb^{96}
Mo^{99}
Nb^{96}
Mo^{99}
Nb^{92m}
Mo^{99}
Nb^{96}
Nb^{91m}
Y^{88}
0.5
1.0
1.5
2.0
Eγ (MeV)

Figure 5.

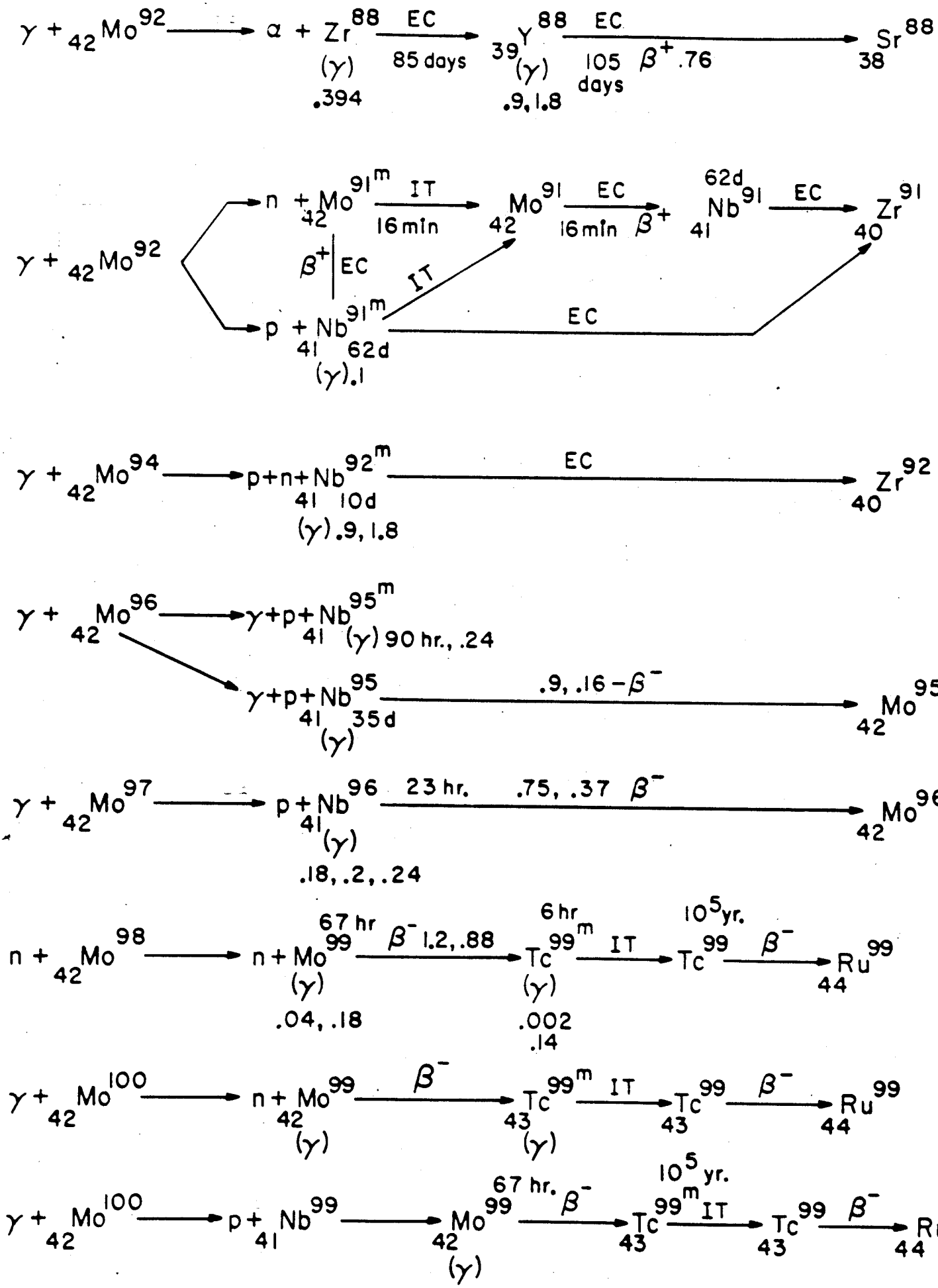
γ + 42Mo92 → α + Zr88 (γ) .394
EC 85 days
39Y88 (γ) .9, 1.8
EC 105 days β+ .76
38Sr88
γ + 42Mo92
n + 42Mo91m IT 16 min 42Mo91
EC 16 min β+ 41Nb91 62d
EC 40Zr91
β+ EC
IT
p + 41Nb91m 62d (γ) .1
EC
γ + 42Mo94 → p+n+41Nb92m 10d (γ) .9, 1.8
EC 40Zr92
γ + 42Mo96 → γ+p+41Nb95m (γ) 90 hr., .24
γ+p+41Nb95 35d (γ)
.9, .16 −β−
42Mo95
γ + 42Mo97 → p + 41Nb96 (γ) .18, .2, .24
23 hr. .75, .37 β−
42Mo96
n + 42Mo98 → n + 42Mo99 67 hr (γ) .04, .18
β− 1.2, .88
43Tc99m (γ) .002 .14
IT
43Tc99 10^5 yr.
β−
44Ru99
γ + 42Mo100 → n + 42Mo99 (γ)
β−
43Tc99m (γ)
IT
43Tc99
β−
44Ru99
γ + 42Mo100 → p + 41Nb99 → 42Mo99 67 hr. (γ)
β−
43Tc99m 10^5 yr.
IT
43Tc99
β−
44Ru99

Figure 6.

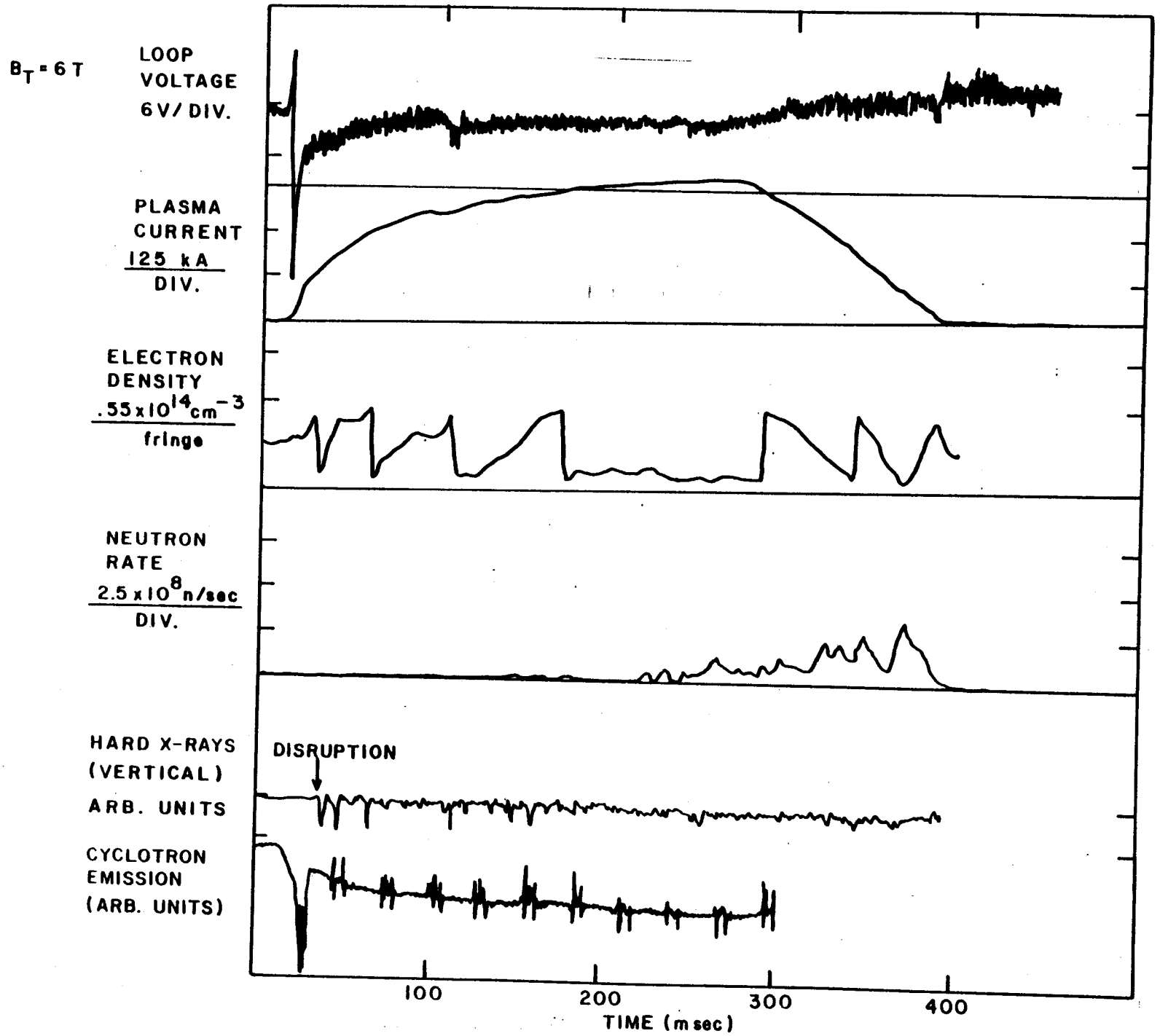
$B_T = 6$ T
LOOP VOLTAGE 6V/DIV.
PLASMA CURRENT 125 kA / DIV.
ELECTRON DENSITY $.55 \times 10^{14} cm^{-3}$ / fringe
NEUTRON RATE 2.5×10^{8} n/sec / DIV.
HARD X-RAYS (VERTICAL) ARB. UNITS
DISRUPTION
CYCLOTRON EMISSION (ARB. UNITS)
100
200
300
400
TIME (m sec)

Figure 7

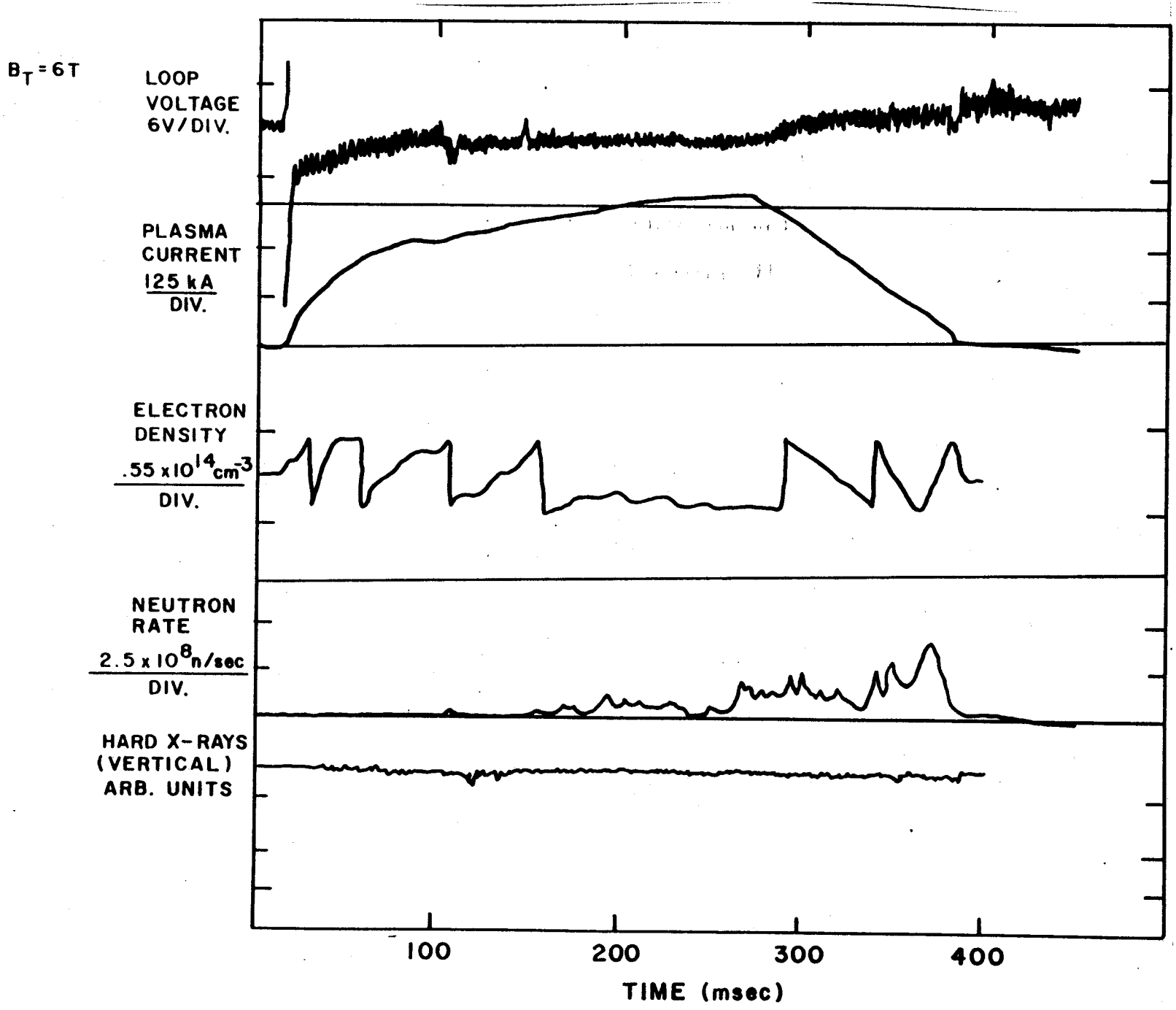
$B_T = 6T$
LOOP VOLTAGE 6V/DIV.
PLASMA CURRENT 125 kA/DIV.
ELECTRON DENSITY $.55 \times 10^{14} cm^{-3}$/DIV.
NEUTRON RATE $2.5 \times 10^{8} n/sec$/DIV.
HARD X-RAYS (VERTICAL) ARB. UNITS
100
200
300
400
TIME (msec)

Figure 8.

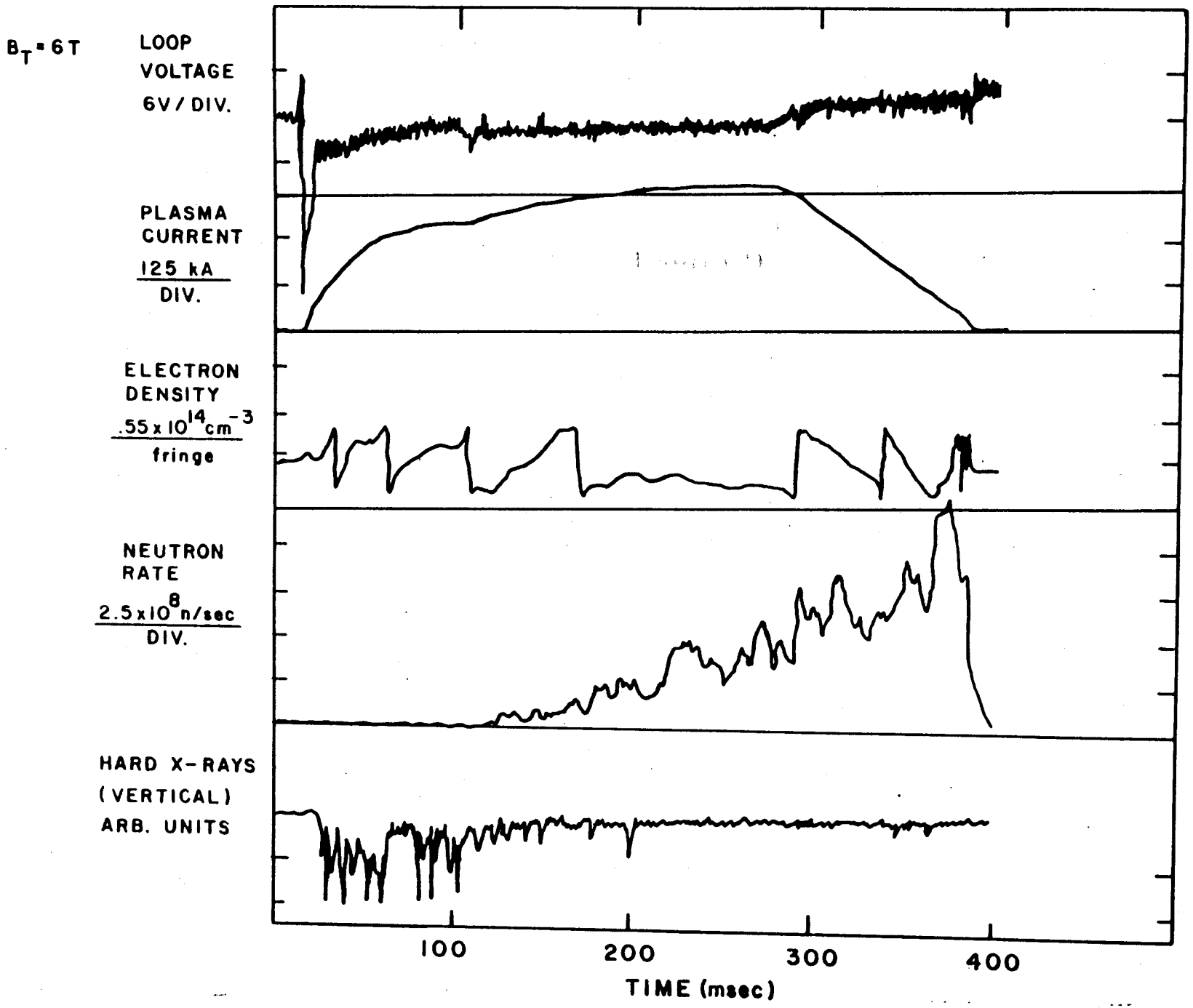
$B_T = 6T$
LOOP VOLTAGE
6V / DIV.
PLASMA CURRENT
125 kA / DIV.
ELECTRON DENSITY
$.55 \times 10^{14} cm^{-3}$ / fringe
NEUTRON RATE
2.5×10^{8} n/sec / DIV.
HARD X-RAYS (VERTICAL) ARB. UNITS
100
200
300
400
TIME (msec)

Figure 9.

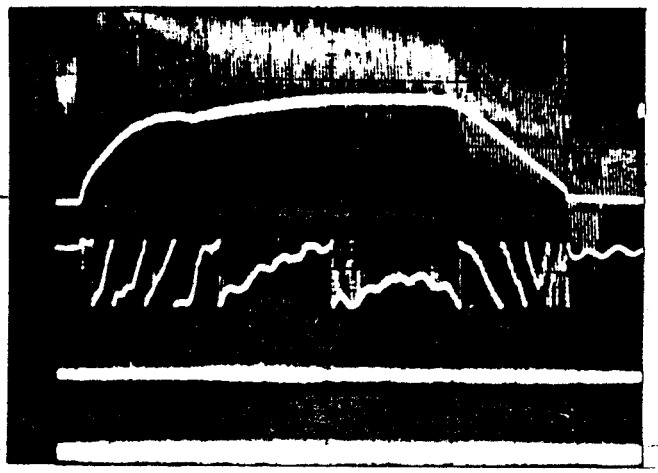
LOOP VOLTAGE
PLASMA CURRENT
ELECTRON DENSITY
HARD X-RAYS (VERTICAL)
NEUTRON RATE
6V/DIV
2^50 kA/DIV.
.55x10^14 cm^-3
Fringe
R_N<6x10^6 n
sec
50 msec/DIV

Figure 10.